Academic Journal of Science and Technology
ISSN: 2771-3032 | Vol. 16, No. 3, 2025

Performance Evaluation and Degradation Study of Anchorage Systems in Prestressed CFRP-Strengthened Concrete Beams under Variable-Amplitude Fatigue

Weifeng Li[1, *]

Nanjing Vocational Institute of Transport Technology, Nanjing, Jiangsu, 211188, China
[*] Corresponding author: Li Weifeng (Email: liweifeng@njitt.edu.cn)

Abstract: This study systematically investigates the performance and fatigue life assessment of anchorage systems in reinforced concrete (RC) beams strengthened with prestressed carbon fiber reinforced polymer (CFRP) plates under variable-amplitude fatigue loading. By integrating experimental testing and numerical simulation, the mechanical behavior and fatigue performance of RC beams strengthened with two different anchorage systems—rigid self-locking anchorage and wedge-clamp anchorage—were comprehensively analyzed. The experimental results demonstrate that prestressed CFRP plates effectively suppress crack propagation, significantly enhance stiffness, and prolong the fatigue life of RC beams. Among the two systems, the wedge-clamp anchorage exhibited superior anchorage performance, achieving a fatigue life of 1.45 million cycles, which represents a 9.2% improvement compared with the rigid self-locking anchorage system (1.31 million cycles). Furthermore, a fatigue life prediction model based on the stress amplitude of prestressed CFRP reinforcement was established and validated, confirming the reliability of the strengthened beams. The findings not only enrich the theoretical framework of prestressed CFRP plate strengthening technology but also provide technical guidance and practical reference for the strengthening and rehabilitation of deteriorated concrete structures such as aging bridges.

Keywords: Prestressed CFRP plates, Reinforced concrete beams, Variable-amplitude fatigue loading, Anchorage system performance, Stiffness degradation, Fatigue life assessment.

1. Introduction

Carbon fibre reinforced polymer (CFRP) plates have been extensively applied in strengthening and rehabilitating deteriorated highway concrete bridges due to their lightweight, high strength, fatigue durability, and corrosion resistance. Prestressed CFRP plate reinforcement, as an active strengthening approach, offers advantages such as ease of construction, significant improvement in load-bearing capacity, minimal damage to girders, and strong economic benefits. Compared with conventional bonded non-prestressed CFRP methods, it allows for fuller utilisation of the superior mechanical properties of CFRP. Since reinforcement alters the structural force distribution, understanding the mechanisms and patterns of such changes is essential to ensure reliable strengthening performance. In recent years, numerous studies have investigated the fatigue behaviour of CFRP-strengthened concrete beams. Analytical models simulating the fatigue process of CFRP-reinforced concrete structures revealed continuous stress redistribution between steel reinforcement and CFRP under fatigue loading, resembling creep-like behaviour [1]. Fatigue testing of CFRP-strengthened beams further demonstrated that stiffness gradually decreases and crack widths expand under repeated high-cycle loading, while the proposed fatigue stiffness calculation models showed good agreement with experimental results [2]. In addition, several researchers have explored the entire fatigue damage process of prestressed CFRP-reinforced members using nonlinear finite element methods [3][4].

Bridge structures are subjected to static loads, moving vehicular loads, and vibration effects, with loading conditions varying over time and often exacerbated by overloading. However, most prior studies primarily address constant-amplitude cyclic loading, while investigations into the behaviour of strengthened members under variable-amplitude loading remain limited. To address this gap, the present study employs two anchorage systems to apply prestressed CFRP plate reinforcement to concrete beam specimens, followed by fatigue testing. The objective is to examine the fatigue response of reinforced members under variable-amplitude cyclic loading and to evaluate their fatigue life.

2. Static Text

2.1. Test preparation

In this study, three concrete test beams were fabricated, each with an overall length of 6000 mm and a clear span of 5400 mm. The cross-sectional dimensions were 350 mm in width and 500 mm in height. The beams were cast using C40-grade concrete, and HRB400 steel bars served as the primary reinforcement. As illustrated in Figure 1, the reinforcement layout consisted of 3Φ16 bars at the top, 3Φ22 bars at the bottom, and 8Φ12 bars as side reinforcement. Stirrups were arranged with Φ10@200 mm spacing over the central 1800 mm region of the span and Φ10@100 mm spacing elsewhere. The experimentally measured material properties of both the concrete and reinforcement are summarised in Tables 1–2.

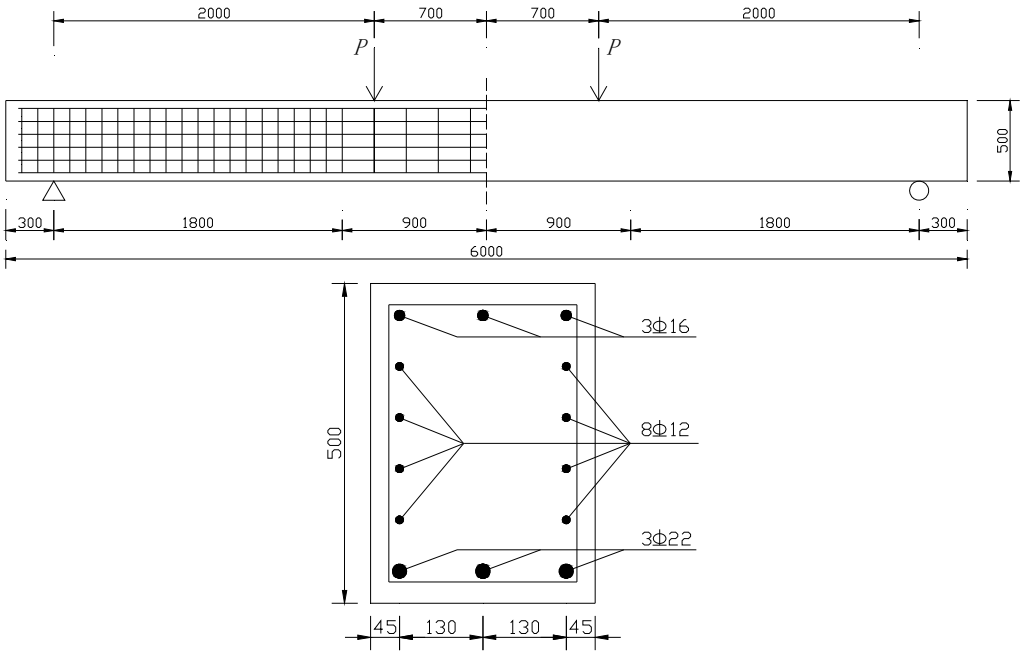

Figure 1. Dimension and Section Reinforcement Drawing of Test Beam(mm)

Table 1. Properties of Concrete

Strength grade	Compressive strength (MPa)	Tensile strength (MPa)	Modulus of elasticity (GPa)
C40	40.8	3.05	32.5

Table 2. Properties of Steel

Type Yield	strength (MPa)	Ultimate strength (MPa)	Modulus of elasticity (GPa)
HRB400	420	610	200

2.2. Anchoring process

For each test girder, a centrally bonded prestressed CFRP plate measuring 50 mm in width, 3 mm in thickness, and 5200 mm in length was applied at the bottom. The tested material properties of the CFRP plate included an elastic modulus of 237 GPa, a tensile strength of 2800 MPa, a linear expansion coefficient of 3.2×10^{-5}, and a Poisson's ratio of 0.17. The control stress during tensioning was set at 1277 MPa. Two different prestressed CFRP anchorage systems were employed for comparison: a "self-locking anchorage system" and a "force-card anchorage system." For both systems, the anchorage length on each side of the CFRP plate was 200 mm. Prior to testing, the plates were tensioned and anchored to the corresponding beams. The specimen designations and details are provided in Table 3.

Table 3. Number and Purpose of Test Piece

Specimen number	Anchorage system	Test application
L1	Unreinforced	Bare Beam Load Capacity Test
A1	Self-locking system	Fatigue test
B1	LIKA system	Fatigue test

2.3. Loading Settings

The location of the loading point of the beam in the fatigue performance test adopts the four-point bending loading method, as shown in Figure 2. During the test, the changes of the beam were carefully observed, and typical damage patterns such as cracking, crack development, yielding of reinforcement, and pulling off of CFRP plate were recorded in time.

Figure 2. Loading Diagram of Test Beam

Based on the static load test results and considering the actual loads experienced by bridge structures, fatigue loading

was applied to the specimens in three stages with a fatigue load ratio of 0.3. The specific load levels and corresponding fatigue cycles are presented in Table 4, with a loading frequency of 4 Hz. In the first stage, representing lower loads, the beam was in the initial cracking state, simulating its behaviour under light loading. The second stage corresponded to intermediate loads, reflecting the specimen's response under moderate service conditions. The third stage involved higher loads, intended to model the structural behaviour under overloading.

Table 4. Fatigue load

Stage	Load up/down Limit value/kN	Number of cycles /10,000 cycles	Type of modelling role
I	80/24	50	Small loads
II	160/48	50	Medium loading
III	280/84	up to destruction	Overloading

To evaluate the mechanical behaviour and flexural capacity of reinforced beams under varying stress amplitudes, an initial static load test was conducted prior to fatigue loading. During the fatigue process, loading was interrupted at 100,000; 300,000; 500,000; 600,000; 800,000; and 1,000,000 cycles for static testing. In each case, the maximum load applied in the static test corresponded to the upper limit of the fatigue load for that stage.

3. Nonlinear Finite Element Analysis

3.1. Reliability Studies

This study develops an advanced numerical model of concrete beams reinforced with CFRP plates using the ANSYS finite element analysis platform, to simulate and analyze the entire static testing process[5]. During the finite element modeling, different element types and constitutive models are employed for various material components: Solid65 elements are used to model the concrete, accounting for cracking and crushing behaviors, with a multilinear isotropic reinforced elastic-plastic constitutive relationship; Shell181 elements represent the mechanical properties of the CFRP plates, utilizing a linear-elastic constitutive model; reinforcement is modeled with Link8 rod elements, which simulate steel reinforcement, applying an ideal elastic-plastic constitutive relationship. All material parameters are derived from experimental data obtained in previous material performance tests to ensure the accuracy and reliability of the model[6].

3.2. Grid division strategy

Regarding the meshing strategy, the concrete beams are discretized using the mapping division method, with a standard cell size of 50 mm to produce a regular 3D hexahedral mesh. The CFRP plates and reinforcement elements also use a 50 mm cell size to ensure mesh compatibility across all components. Rebar modeling is performed via the solid cut-off method, and the bond-slip effect between the rebar and concrete is temporarily neglected. For boundary conditions, node constraints are applied at the support locations: a fixed hinge support restricts movements in all three directions (UX, UY, UZ), while a sliding hinge support restricts movements in the UY and UZ directions. To accurately replicate actual working conditions, the self-weight of the beam is incorporated into the model[7]. Additionally, the concentrated load is converted into a surface load applied in the loading area to prevent stress concentration issues.

3.3. Interface Connection Simulation

To address the key technical challenge of accurately simulating the interface connection between the CFRP plate and concrete, this study introduces an improved modeling approach[8]. Unlike the conventional bonding method using the GLUE command, this model reflects the actual force characteristics of the prestressed CFRP plate. It employs the node degree of freedom coupling (CP command) method to rigidly connect the nodes in the anchorage zone at the end of the CFRP plate with the corresponding concrete nodes, thereby more realistically capturing their combined mechanical behavior[9]. The prestressing force is simulated using a temperature stress approach, which mimics the tensioning process through a graded cooling method. This results in an effective prestressing force of 1500 MPa, accounting for a 6% prestress loss. This modeling technique effectively addresses the interface connection distortion issues commonly encountered in traditional simulations and greatly enhances analysis accuracy. Figure 3 illustrates the overall finite element model, including detailed meshing and boundary condition configurations, providing a solid foundation for subsequent parametric studies and verification of the results.

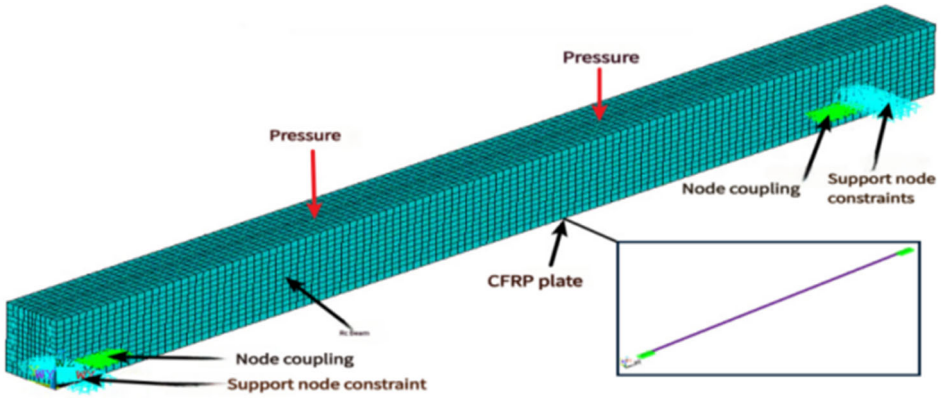

Figure 3. Finite Element Model of Strengthened Beam

4. Analysis of Test Results

4.1. Crack Development and Damage Patterns

Stage I: After the initial static load test, a few microcracks appeared in the concrete beams. In subsequent static loading, the number of cracks increased slightly, but their widths showed no significant change.Stage II: Both the width and height of cracks increased, and new cracks developed during later tests, although their widening remained limited.Stage III: Crack width and height continued to grow. Cracks in the pure bending zone became more concentrated, while additional cracks were also observed in the bending–shear region.

In all static load tests, cracks closed after unloading, demonstrating that prestressed CFRP plates bonded to the beam bottom effectively restrained crack development [10]. Previous studies reported that cracks in unreinforced beams typically form only in high-moment regions, appear earlier, propagate more quickly, and are fewer in number but larger in width. In contrast, the present tests showed that beams reinforced with prestressed CFRP plates developed denser cracks of smaller width, distributed across both the pure bending and bending–shear zones. This indicates that under fatigue loading, the CFRP reinforcement helps fully mobilise the mechanical properties of reinforced concrete beams [11].

For specimen A1, rapid stiffness degradation was observed after 1.3 million fatigue cycles, as indicated by a sharp drop in load capacity. At 1.31 million cycles, failure occurred with a loud noise. As illustrated in Figure 4(a), one tensile bar and one distribution bar fractured, the beam split into two segments, and the CFRP plate slipped out of the rigid self-locking anchorage. Analysis of deformation, strain, and other data suggests that after one million cycles, anchorage relaxation occurred in the rigid self-locking system, leading to increased deformation at equal loads, higher stress amplitude in the reinforcement, and eventual fatigue rupture of the rebar. The CFRP plate was then pulled out of the anchorage, resulting in complete fracture of the specimen.

Specimen B1 failed at 1.43 million fatigue cycles, also accompanied by a loud noise. As shown in Figure 4(b), three tensile bars and two distribution bars fractured, the beam split into two sections, and the CFRP plate was crushed. Unlike specimen A1, the LIKA anchorage system maintained stable performance throughout fatigue loading and remained effective until final failure. The ultimate damage mechanism was attributed to cumulative fatigue deterioration of the reinforcement, which eventually caused fatigue rupture.

(a) Specimen A1

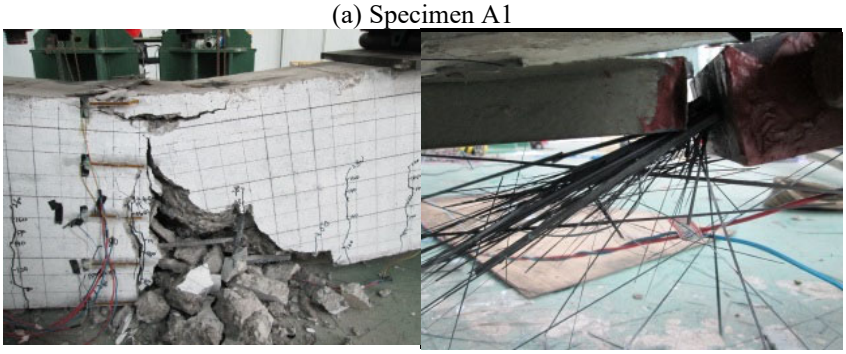

(b) Specimen B1

Figure 4. Failure mode of specimen

4.2. Rigidity Degradation

The load–midspan displacement curves of specimens A1 and B1 after the initial static load test and following 500,000, 1,000,000, and 1,200,000 fatigue cycles are presented in Figs. 5(a) and 5(b). The results indicate that midspan deflections under the same static load increased progressively with the number of fatigue cycles, reflecting continuous stiffness degradation. In the early fatigue stage, residual deflection developed more rapidly. After approximately 1 million cycles, the deflection growth of the strengthened beams accelerated, and stiffness loss became more pronounced. Nevertheless, the slopes of the load–deflection curves remained nearly constant across different fatigue stages, showing that the reinforced beams largely preserved linear elastic behavior [12].

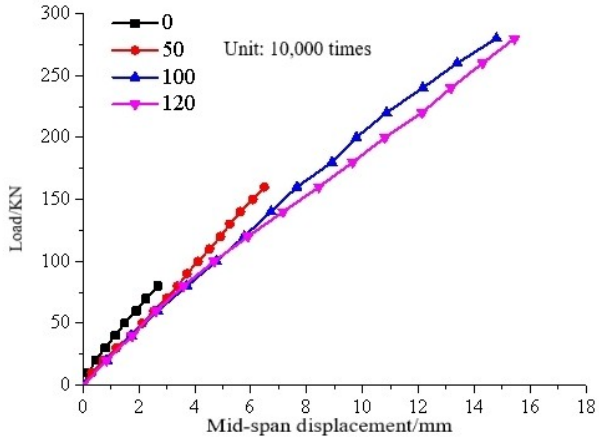

(a) Specimen A1

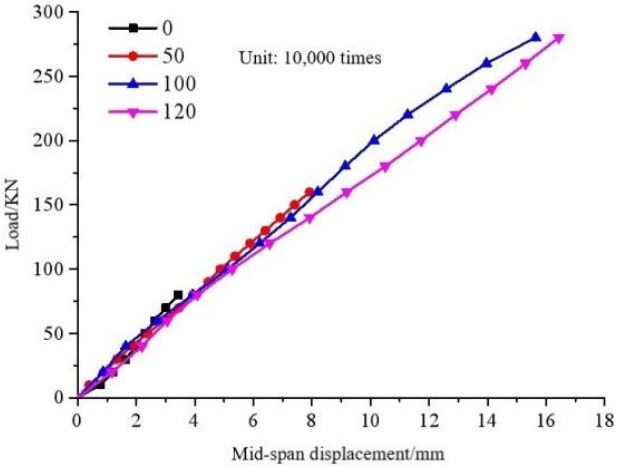

(b) Specimen B1

Figure 5. Load-Mid Span Displacement Curves of Reinforced Beams

The stiffness of the specimen in the four-point bending test can be calculated from the following equation:

$$B = \frac{\Delta F}{\Delta f}\left[\frac{\left(L-L_f\right)^3}{24}+\frac{\left(2L-L_f\right)\left(L-L_f\right)}{16}L_f\right] \quad (1)$$

Where: B denotes the bending stiffness of the specimen; F is the applied load; f is the mid-span displacement; the specimen span is L = 5400 mm, and the distance between the two loading points is 1400 mm.

The stiffness degradation curves of specimens A1 and B1 under fatigue loading, calculated using Eq. (1), are presented in Fig. 6. Results show that with increasing fatigue cycles, the bending stiffness of both specimens exhibits an approximately linear decline, attributed to the progressive accumulation of fatigue damage [13].

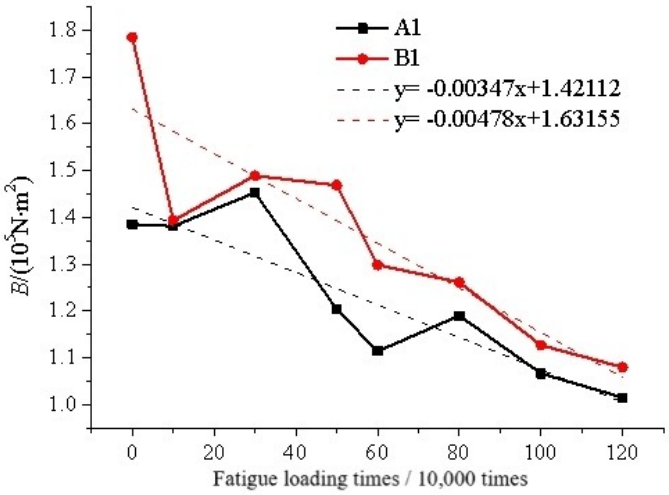

Figure 6. Stiffness Performance Degradation Curve

The bending stiffness was obtained by linearly fitting the data to the number of fatigue loadings:

$$y_{A1} = -0.00347x + 1.42112$$
$$y_{B1} = -0.00478x + 1.63155 \quad (2)$$

Where:, is the flexural stiffness of specimens A1 and B1 respectively (105N-m2); is the number of fatigue loading (10,000 times).

However, Fig. 6 shows that the bending stiffness of specimen A1 after 300,000 and 800,000 fatigue cycles, as measured in the static load test, was higher than in the preceding test. A similar anomaly was also observed for specimen B1 after 300,000 cycles. This phenomenon can be attributed to the increase in the number of cracks and the corresponding reduction in crack width under fatigue loading, which leads to a more uniform stress distribution in the specimen [14].

4.3. Adaptive Change

The strain variation curves of the mid-span concrete at the beam bottom, the CFRP plate, and the tensile reinforcement of specimens A1 and B1 after different fatigue load cycles are presented in Figs. 7–9. In each figure, part (a) illustrates the strain response of specimen A1, while part (b) depicts that of specimen B1.

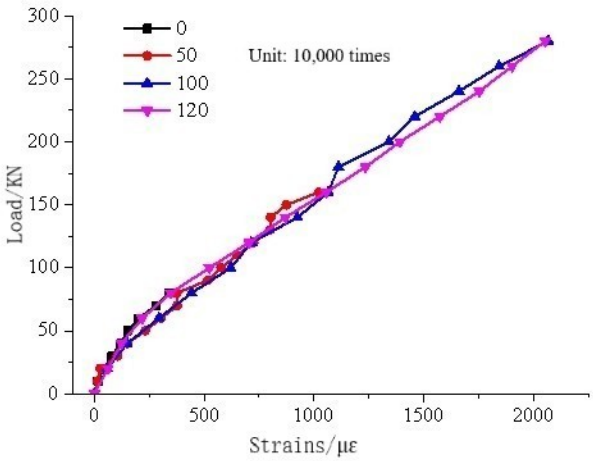

(a) Specimen A1

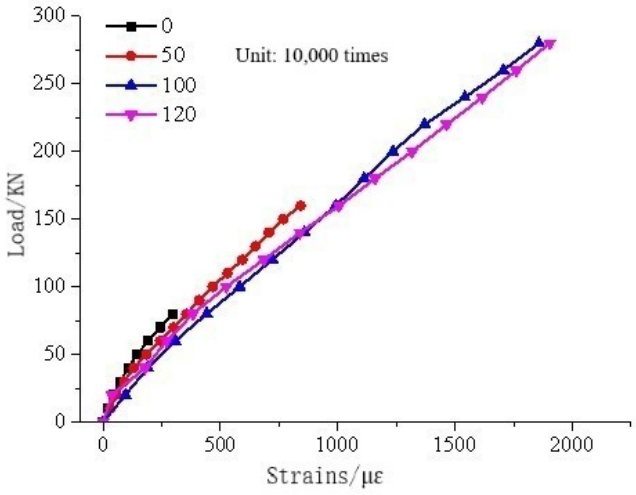

(b) Specimen B1

Figure 7. Concrete Strain Curve at The Bottom of Mid-Span Beam

As shown in Fig. 7, when the applied load is relatively small, the strain curves of the concrete at the girder bottom after different fatigue cycles remain close. However, as the number of cycles increases, the mid-span bottom concrete strain gradually rises, reflecting the accumulation of fatigue damage [15].

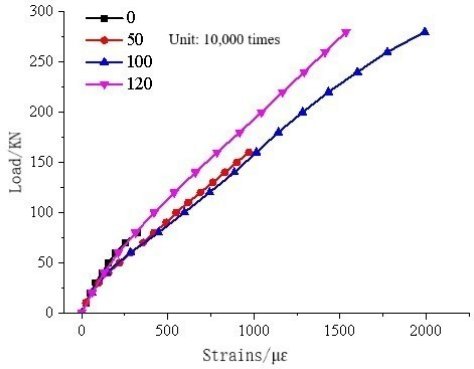

(a) Specimen A1

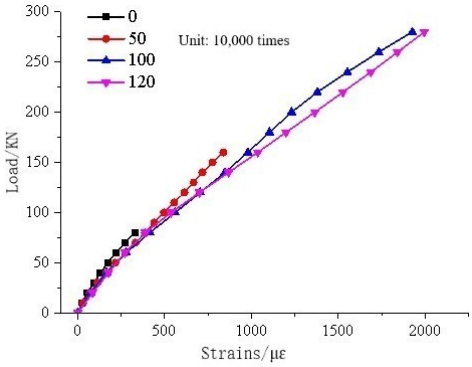

(b) Specimen B1

Figure 8. Strain Curve of CFRP Plate at The Bottom of Mid-Span Beam

As shown in Fig. 8, the CFRP plate strain curves remain relatively close when the fatigue cycles are below one million, but overall the strain increases with additional cycles. Notably, in Fig. 8(a), after 1.2 million cycles, the CFRP plate strain under the same load is lower than that observed after 500,000 and 1,000,000 cycles. Based on the final failure pattern, this behavior is attributed to slight slippage of the CFRP plate ends from the rigid self-locking anchorage under the overloading conditions of Stage III. In contrast, Fig. 8(b) indicates that the CFRP plate strain consistently rises with increasing cycles, demonstrating that the LIKA anchorage system performs reliably under fatigue loading without slippage.

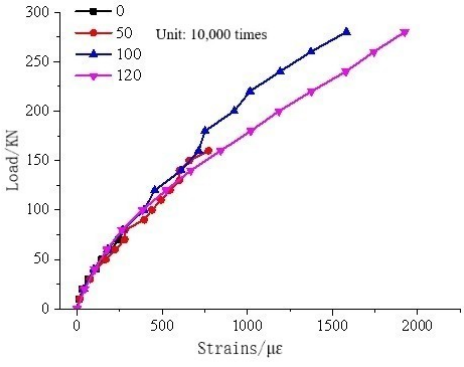

(a) Specimen A1

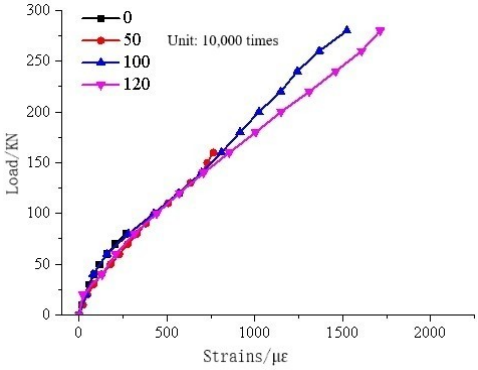

(b) Specimen B1

Figure 9. Strain Change Curve of Main Bar Under Tension in Mid-Span

As shown in Fig. 10, the strain in the mid-span tensile reinforcement generally increases with the number of fatigue cycles. In Fig. 10(a), when the cycles are below one million, the strain variation under the same load is minimal; however, after 1.2 million cycles, the strain at the span-center section rises sharply. This is attributed to minor slippage of the CFRP plate ends from the rigid self-locking anchorage during Stage III overloading, which amplifies the stress in the tensile reinforcement. In contrast, Fig. 10(b) shows that after 1.2 million cycles, the strain in the mid-span tensile reinforcement of specimen B1 increases only slightly compared with earlier stages, and the growth is less pronounced than in specimen A1. This indicates that the force-card anchorage system exhibits superior performance under fatigue loading compared with the rigid self-locking system.

5. Fatigue Life Analysis of Reinforced Beams

Experimental results and related research indicate that fatigue failure of CFRP-strengthened concrete beams is primarily governed by the fatigue fracture of the main reinforcement, with the stress amplitude in the reinforcement serving as the key factor in determining the fatigue life of CFRP-strengthened members. Thus, reinforcement stress can be used as a basis for predicting the fatigue life of such beams.

For specimens A1 and B1, fatigue lives were 1.3 million and 1.43 million cycles, respectively, both below 2 million cycles. This reduction is attributed to the higher stress amplitude applied during Stage III fatigue loading, which simulated overload conditions and demonstrated the significant influence of overloading on fatigue life. The strain values of the mid-span tensile reinforcement at each stage were used to derive the stress amplitude of the steel bars, and the calculation adopts the formula corresponding to a stress ratio of 0.3, namely:

$$\lg N_f = 34.31736 - 12.56013 \lg \Delta\sigma_m \tag{3}$$

According to the Code for the Design of Concrete Structures, the fatigue stress amplitude limit for HRB400 reinforcement at a load ratio of 0.3 is 145 MPa. The code conservatively defines the fatigue life under this stress amplitude as 2 million cycles. Based on the cumulative fatigue damage theory, variable-amplitude fatigue loading can be transformed into an equivalent constant-amplitude load[16], expressed by the following formula:

$$\sum \frac{n_i}{N_i} = \frac{n_m}{N_m} \tag{4}$$

Based on Equations (3) and (4), the variable-amplitude fatigue load in the test is converted into an equivalent constant-amplitude load with a steel bar stress amplitude of 145 MPa, and the corresponding fatigue life is calculated. The results show that specimen A1 has a fatigue life of 8 million cycles >> 2 million cycles, while specimen B1 reaches 12 million cycles >> 2 million cycles. These findings confirm that the tested structures fully satisfy the code requirements.

6. Conclusion

In this paper, the mechanical behaviour of RC beams reinforced with prestressed CFRP plates under variable fatigue loading is revealed through systematic experimental study and numerical analysis. It is shown that a reasonable choice of anchorage system is a key factor to ensure the reinforcement effect, and the LIKA anchorage system exhibits more stable working performance under long-term fatigue loading. The established fatigue life prediction model provides a quantitative assessment tool for engineering practice. Future research can further consider the effects of actual working conditions such as environmental corrosion and load spectrum variability to improve the design theory and method system of prestressed CFRP reinforcement technology. This study provides an important technical support for the reinforcement of concrete structures such as bridges.

References

[1] R. Qin et al., “Understanding on the creep behavior of fiber reinforced polymer via fiber/matrix interaction,” Constr. Build. Mater., vol. 451, p. 138875, 2024.

[2] W. Wu et al., “Effect of high-stress level loads on the fatigue performance of GFRP-RC beams,” Compos. Part C open Access, vol. 12, p. 100399, 2023.

[3] X. Guo, Y. Wang, P. Huang, and Z. Chen, “Finite element modeling for fatigue life prediction of RC beam strengthened with prestressed CFRP based on failure modes,” Compos. Struct., vol. 226, p. 111289, 2019.

[4] Koch, M. Zscheyge, K. Tittmann, and M. Gude, “Numerical fatigue analysis of CFRP components,” Compos. Struct., vol. 168, pp. 392–401, 2017.

[5] A. Sakbana and M. Mashreib, “Finite element analysis of CFRP- reinforced concrete beams,” Rev. Ing. Constr., vol. 35, no. 2, 2020, doi: 10.4067/S0718-50732020000200148.

[6] T. Gu, N. Liu, Z. Feng, X. Sun, and X. Meng, “Research on equivalent modeling and model testing verification methods for material mechanics parameters of TXV structure,” Microelectron. Reliab., vol. 163, p. 115545, 2024.

[7] S. B. B. Aval, M. Ghabdian, M. Noori, and W. A. Altabey, “Simultaneous effect of temperature, shrinkage, and self-weight creep on RC beams: a case study,” Proc. Inst. Mech. Eng. Part L J. Mater. Des. Appl., vol. 236, no. 5, pp. 1020–1036, 2022.

[8] Y. Bounjoum, o. Hamlaoui, M. K. Hajji, K. Essaadaoui, J. Chafiq, and M. A. El Fqih, “Exploring damage patterns in CFRP reinforcements: Insights from simulation and experimentation,” Polymers (Basel)., vol. 16, no. 14, p. 2057, 2024.

[9] A. Aloisio, R. Alaggio, and M. Fragiacomo, “Dynamic identification and model updating of full-scale concrete box girders based on the experimental torsional response,” Constr. Build. Mater., vol. 264, p. 120146, 2020.

[10] H.-T. Wang, Z.-N. Bian, M.-S. Chen, L. Hu, and Q. Wu, “Flexural strengthening of damaged steel beams with prestressed CFRP plates using a novel prestressing system,” Eng. Struct., vol. 284, p. 115953, 2023.

[11] X. Li, J. Deng, Y. Wang, Y. Xie, T. Liu, and K. Rashid, “RC beams strengthened by prestressed CFRP plate subjected to sustained loading and continuous wetting condition: Time-dependent prestress loss,” Constr. Build. Mater., vol. 275, p. 122187, 2021.

[12] F. Aslani, Y. Gunawardena, and A. Dehghani, “Behaviour of concrete filled glass fibre-reinforced polymer tubes under static

and flexural fatigue loading," Constr. Build. Mater., vol. 212, pp. 57–76, 2019.

[13] M. T. A. Ansari, K. K. Singh, and M. S. Azam, "Fatigue damage analysis of fiber-reinforced polymer composites—A review," J. Reinf. Plast. Compos., vol. 37, no. 9, pp. 636–654, 2018.

[14] B. G. Charalambidi, T. C. Rousakis, and A. I. Karabinis, "Fatigue behavior of large-scale reinforced concrete beams strengthened in flexure with fiber-reinforced polymer laminates," J. Compos. Constr., vol. 20, no. 5, p. 4016035, 2016.

[15] S. Venkatachalam and H. Murthy, "Damage characterization and fatigue modeling of CFRP subjected to cyclic loading," Compos. Struct., vol. 202, pp. 1069–1077, 2018.

[16] Y.-E. Guo, D.-G. Shang, D. Cai, T. Jin, and D.-H. Li, "Fatigue life prediction considering temperature effect for carbon fibre reinforced composites under variable amplitude loading," Int. J. Fatigue, vol. 168, p. 107442, 2023.